A report on

Tribological characterisation of brake block material and steel tribopairs under dry and icy conditions

Submitted to

Transportstyrelsen

By

Leonardo Pelcastre

Lisa-Marie Weniger

Jens Hardell

Division of Machine Elements

Luleå University of Technology

971 87 Luleå

October 2021

Table of Contents

1. Introduction

Over the past years, a problem associated with sudden loss of braking has been observed in winter conditions for trains equipped with tread brakes and composite brake blocks (CBB). The problem is more significant at temperatures below -15 °C and in combination with fly-off snow. This problem is not occurring for trains equipped with the traditional cast iron brake blocks. Due to the severe nature of this problem and potential risk for incidents and accidents, the Swedish Transport Agency (Transportstyrelsen) is carrying out different activities to find solutions. One such activity is a more detailed understanding of the friction mechanisms between brake block and wheel, with special emphasis on the effect of sub-zero temperatures as well as presence of ice/snow/water between brake block and wheel on the friction behaviour. Furthermore, it is also of interest to find test methods that can be used for evaluation of new developed brake materials under well-controlled laboratory conditions. One observation from field tests is the presence of an ice layer on the friction surface of the brake block. This is believed to be one cause for the reduced friction and hence loss of braking performance. It is also of interest to understand if different brake materials have different probability of forming ice layers due to their water absorption properties. The work has been carried out at the Division of Machine Element, Luleå University of Technology (LTU), and was commissioned by Transportstyrelsen.

1.1. Background to brake block materials and the tribosystem

The issue of sudden loss of braking performance is typically not observed when using cast iron brake blocks. The conventional material is a pearlitic cast iron with graphite nodules denoted as P10, which gives good friction performance and high thermal conductivity. The advantages with cast iron are [1]:

- Friction is independent of environmental conditions and material supplier,
- Good thermal conductivity and 20-30% of the frictional heat is dissipated via the brake block,
- Smaller wheel flats are worn away during braking,
- The wheel surface is worn and maintains a constant adhesion level.

The main disadvantage with cast iron as brake material is that friction depends on both load and speed (higher friction at low speed [2]) and that the noise level from the train increases.

When it comes to composite brake blocks (CBB) there are three main types [3]:

- Type K - material that gives high friction and is either organic or sintered,
- Type L - material that give medium friction,
- Type LL - material that gives low friction, comparable to cast iron, and is either organic or sintered.

The reduced thermal conductivity for CBB materials implies that more frictional heat has to be dissipated via the wheel to prevent excessive contact temperatures and martensite formation in the near surface region of the wheel tread.

The wheel material is a pearlitic steel (UIC 812-3 R7/EN 13262 ER7) with a carbon content of 0.52 wt.% and a yield strength of >540 MPa and an ultimate tensile strength of 860-980 MPa [4]. The tread of the wheel is sometimes heat treated (R7T) or even the entire wheel (R7E).

When analysing the braking performance of the brake block – wheel system, it is important to understand the fundamental concept of a tribosystem. As shown in Figure 1, the brake block – wheel tribosystem consist of four main elements. The first element is the brake block, the second is the wheel, the third is the interfacial medium present between the brake block and wheel (e.g. dust, ice, water, etc.) and the fourth element is the surrounding environment which is air, humidity etc.

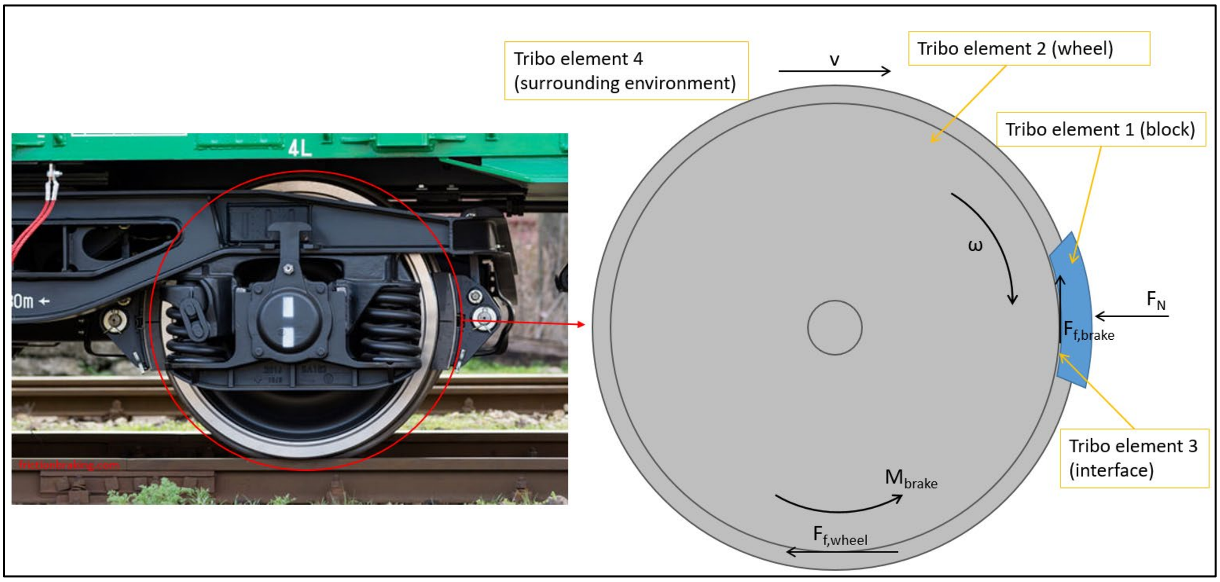

Figure 1. The brake block – wheel tribosystem.

It is also equally important to consider that friction and wear are not intrinsic material properties, such as e.g. hardness, but a system response, which depends on a large number of variables. A schematic of the brake block – wheel contact is shown in Figure 2 together with the main parameters that will affect friction during braking. The surrounding temperature does not have a direct relation to friction but indirectly affect parameters that can have an impact on the resulting tribological system response.

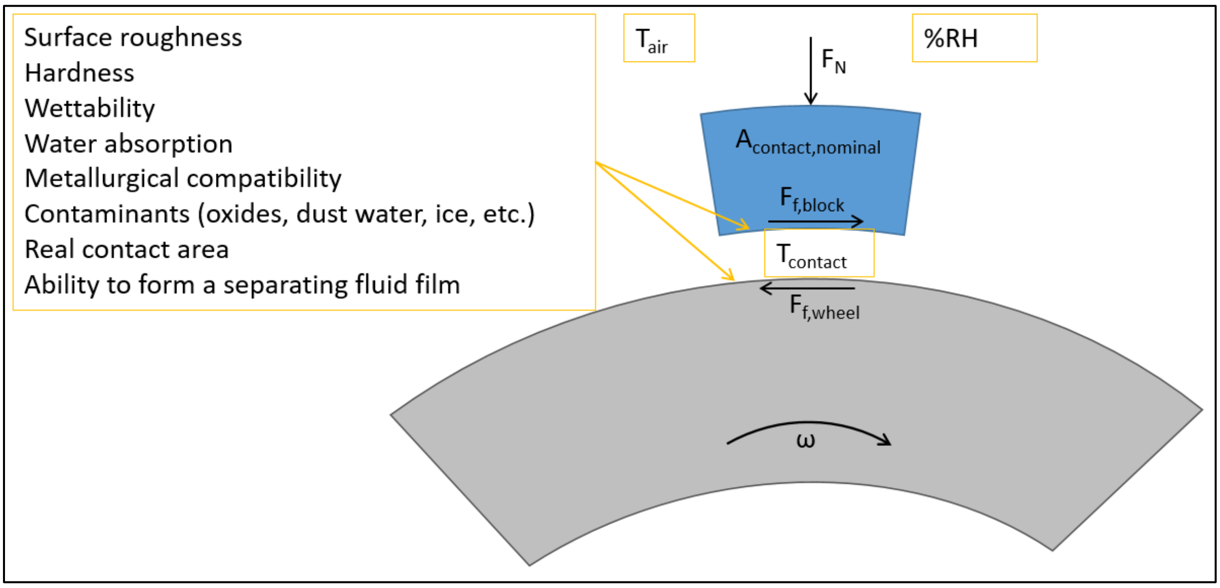

Figure 2. The parameters that affect friction in the brake block – wheel tribosystem.

The contact pressure is an important parameter that determines, together with sliding speed and coefficient of friction, the friction power and hence contact temperature. Typical contact pressures for different brake block materials and wheel are given in Table 1. As seen, for type K blocks the sintered versions give higher friction against the wheel compared to the organic (normal load is reduced to maintain the same friction force). The type LL blocks give lower friction and require a higher normal load to achieve the same friction force. The organic and sintered type LL gives the same friction performance.

Table 1. Brake block materials and typical contact pressures at low and high axle loads.

Brake block	Material	Type	Min. contact pressure [MPa]	Max. contact pressure [MPa]
Jurid 822	Organic CBB	K (high friction)	0.20 (axle load 4.7 tonne)	0.76 (axel load 22.5 tonne)
CoFren C810	Organic CBB	K (high friction)	0.20 (axle load 4.7 tonne)	0.76 (axel load 22.5 tonne)
CoFren C333	Sintered CBB	K (high friction)	0.14 (axel load 4.7 tonne)	0.59 (axel load 22.5 tonne)
Icerail/Becorit IB116*	Organic CBB	LL (low friction)	0.15 (axel load 3.6 tonne)	1.25 (axel load 22.5 tonne)
CoFren C952-1	Sintered CBB	LL (low friction)	0.15 (axel load 3.6 tonne)	1.25 (axel load 22.5 tonne)
Cast iron P10	Cast iron	Friction corresponding to LL	0.15 (axel load 3.6 tonne)	1.25 (axel load 22.5 tonne)

Since the coefficient of friction varies between different brake block materials, the braking force (normal load) is changed to have the same friction force. As shown in Figure 3, the braking moment (M_{brake}) is therefore constant irrespective of brake block material resulting from the friction force also being constant and therefore the friction power per unit area becomes constant. This means that the frictional heat generation is theoretically the same regardless of the brake block material. There may of course be exceptions to this due to variations in e.g. contact area due to different wear and running-in properties of the brake block materials.

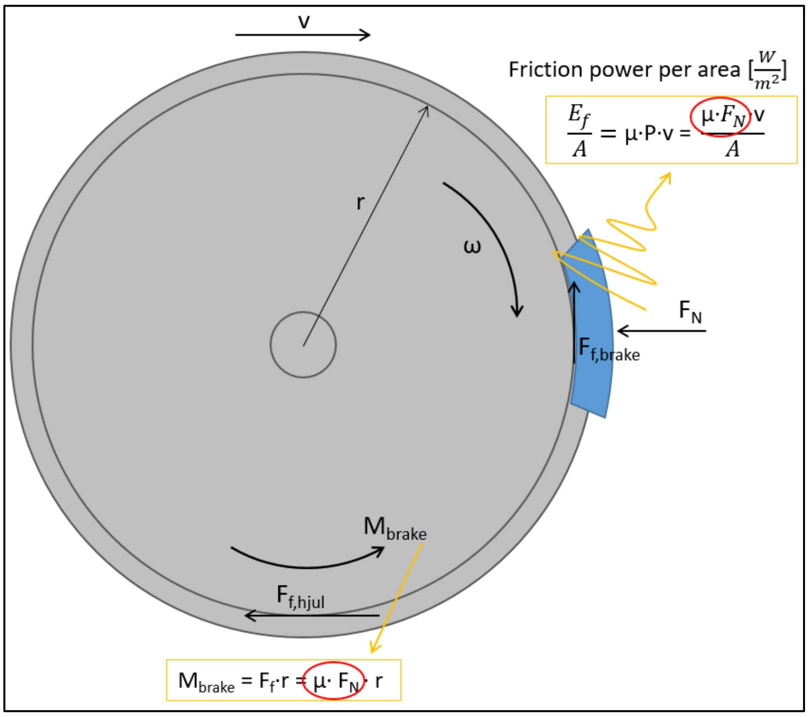

Figure 3. Brake block – wheel tribosystem highlighting the parameters affecting friction power per area and the frictional heating.

1.2. Field experience and hypotheses about the ice formation

The following information is a summary based on field experience from train operators (Hector Rail and Green Cargo), the Swedish Transport Agency, and members of the brake system task force working with friction problems in winter climate. The information was obtained during work group meetings on 18 January, 10 February, and 10 March 2021.

The loss of braking performance occurs when CBB of type K or LL are used and when the wagons are empty or lightly loaded (low braking force). The problem is particularly severe at temperatures below - 15 °C and with fly-off snow present [3]. The problem arises both directly after starting the train as well as during running.

Two main hypotheses are presented to explain the loss of braking performance:

1. An ice layer is formed on the functional surface of the brake block, which reduces friction through a thin water film that is formed when the block is loaded against the wheel.
    a. This is a likely mechanism if the braking performance is low immediately when the brakes are engaged and if there is an improvement in braking performance resulting from the ice layers breaking up and being removed.
    b. It would suggest that loss of braking performance occurs even at low speeds.
    c. Any ice formed on the wheel will likely be removed immediately when the train starts to move due to the high contact pressure against the rail.
2. If the entire brake block is enclosed in ice, the melting of this ice (from frictional heating) will generate water that can enter the contact between the brake block and wheel. Since the wheel surface, in case of CBB, is very smooth, it increases the probability of generating a hydrodynamic water film that separates the two surfaces.
    a. If there is a gradual loss of braking performance, this may be a possible mechanism.
    b. Should not occur at low speeds since hydrodynamic film formation depends on speed.

Two important aspects regarding ice layer formation are:

1. Surface roughness of the wheel:
    - During braking with cast iron brake blocks, the wheel surface becomes rough with up to millimetre sized amplitude variations. This implies that any ice formation on the cast iron brake block will be quickly removed due to high local contact pressures.
    - The wheel surface when using CBB is very smooth and does not provide the same possibility to remove any ice.
2. Thermal conductivity of the brake blocks:
    - Typical thermal conductivity for different blocks are:
        - Cast iron 50-70 W/m/K
        - CBB sintered 20-30 W/m/K
        - CBB organic 1-5 W/m/K
    - A higher thermal conductivity will result in a higher average temperature of the block leading to reduced risk of water/snow freezing on the surface and prevention of the entire block being enclosed in ice.
    - If the ice layer on the brake block is not fully covering the entire friction surface, direct contact between block and wheel occurs, leading to frictional heating and subsequent melting of the ice. This process is faster with higher thermal conductivity.

Some examples of ice formation on Jurid 822 (CBB type K organic) and CoFren C333 (CBB type K sintered) are shown in Figure 4. The photos are taken at the same occasion in the same train set where some wagons were equipped with organic CBB (Jurid 822) and others with sintered CBB (C333). The train is operated between Piteå and Murjek in northern Sweden and operates fully loaded in one direction and empty on the return trip. It is obvious that the sintered CBB does not result in any ice formation whereas for the organic material, the entire brake block is encapsulated in ice.

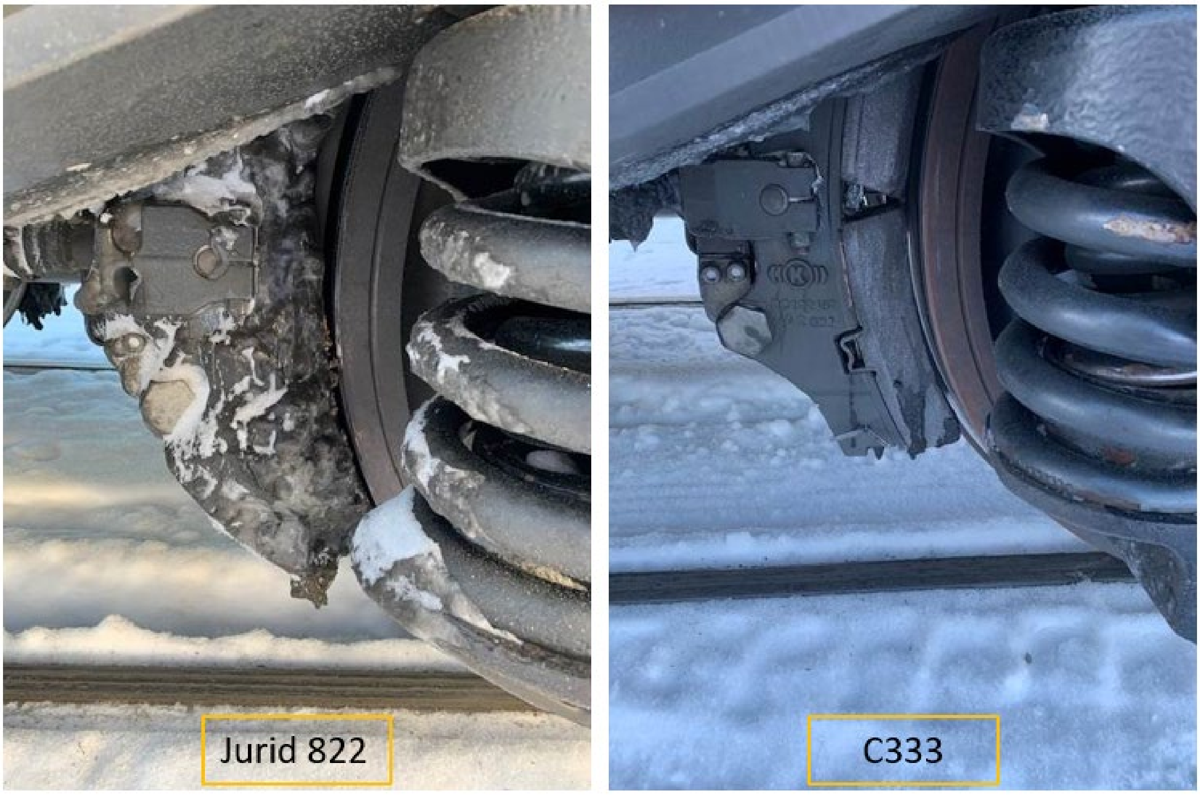

Figure 4. Ice formation on organic (Jurid 822) and sintered (C333) CBB in the same train set. Photo courtesy of Petter Hydén, Hector Rail.

Figure 5 shows two other Jurid 822 brake blocks in the same train set as those shown in Figure 4. It should be noted that ice formation is not only limited to the brake block but also occurs on the springs in the bogie suspension as well as parts of the wagon frame. This suggests that the frictional heat results in substantial melting of fly-off snow leading to water splashing around and freezing on the surrounding cold surfaces.

In Figure 6, a side view of the ice layer as typically seen on the friction surface on the brake block is shown. This particular layer is relatively thick and covers the entire block. Thinner layers are also found. However, this photograph does not show the fraction of the contact area of the brake block that is covered.

The ice layer formation occurs primarily for organic CBB and is observed after standstill, during operation while exercising the brakes, and when the wheel is hot and the brake block is cold (organic CBB). When the train is fully loaded and a high brake force is used, the ice is more easily removed. In case of an empty train, and hence a lower braking force (Table 1), the ice is difficult to remove and results in the loss of braking performance.

Figure 5. Ice formation of organic CBB Jurid 822. Photo courtesy of Petter Hydén, Hector Rail.

Figure 6. Ice layer formation on the friction surface of organic CBB Jurid 822. Photo courtesy of Petter Hydén, Hector Rail.

It is clear that the loss of braking performance in winter climate when using CBB brake blocks for tread brakes on train wagons is a complex question. More comparable data and basic knowledge about the friction performance of CBB materials is required to understand why some materials fail under certain conditions and ultimately to enable judicious selection of appropriate materials for tread brake systems in winter conditions.

2. Aim and Objectives

The aim of this work is to characterise the surface properties as well as the friction and wear behaviour of five different brake block materials during sliding against steel using different tribological test methods.

The specific objectives are to:

- Measure surface roughness of brake block materials and steel counter surface,
- Measure water absorption for the composite brake block materials,
- Perform friction and wear tests in dry/room temperature conditions using a block-on-ring test setup,
- Carry out friction measurements at sub-zero temperature in humid environment and in vacuum using a pin-on-disc test setup.

3. Experimental procedure

This section describes the experimental methods and materials analysed.

3.1 Test materials

The experimental materials were five different brake block materials; cast iron as reference, two organic CBB (IB116* type LL and Jurid 822 type K), and two sintered CBB (C952-1 type LL and C333 type K). These were machined from new brake blocks using band saw, turning, and milling. Specimens for block-on-ring and pin-on-disc tests were manufactured.

The counter specimens (rings and discs) were machined from a used train wheel made from ER7 steel. The hardness of the wheel steel specimens at the test surface was 245 $HV_{0.3}$ for the rings and 270 $HV_{0.3}$ for the discs. The difference in hardness is a result of their dimensions and where in the wheel tread the specimens were taken from, as well as the orientation of the specimens when extracted. Since the specimens were taken from a worn train wheel, the hardness was higher near the surface due to strain hardening that occurs during operation. The contact surface in the tribological tests with the block-on-ring, was within the bulk of the wheel, whereas the contact surface of the discs was near the surface of the wheel, and thus slightly harder. Figure 7 shows a schematic representation of where the specimens were taken from.

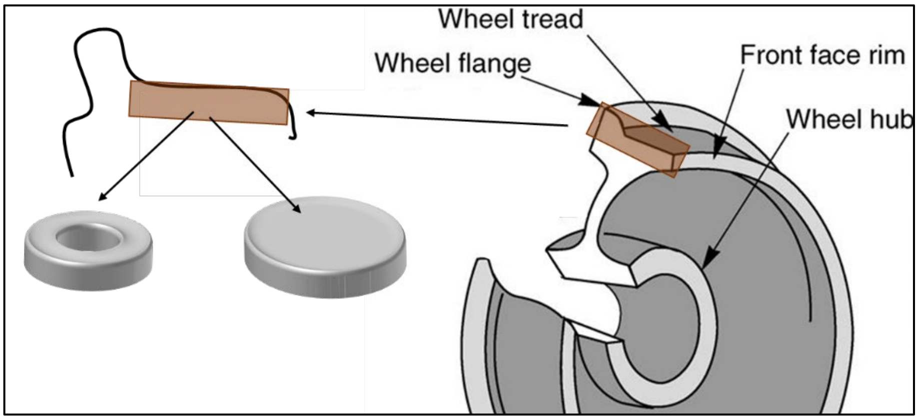

Figure 7. Schematic representation of where in the train wheel the specimens were extracted from.

3.2 Block-on-ring tests

The appearance of the experimental materials and test specimens are shown in Figure 8. The dimensions of the block specimens were 11.6 x 9.75 x 6.3 mm^3. The ring specimen dimensions were Ø35 mm and width 8.8 mm.

Figure 8. The block specimens and the ring counter surface for the block-on-ring tests.

For the friction and wear studies at room temperature, a CETR UMT tribometer with a block-on-ring test setup was employed. The tribometer consists of an upper carriage and a lower rotational drive, Figure 9. The upper carriage can be controlled to move vertically up and down and consists of a load cell that can measure both the friction force and the applied normal force. The lower part of the tribometer has a rotational drive with a shaft onto which the ring specimen is mounted.

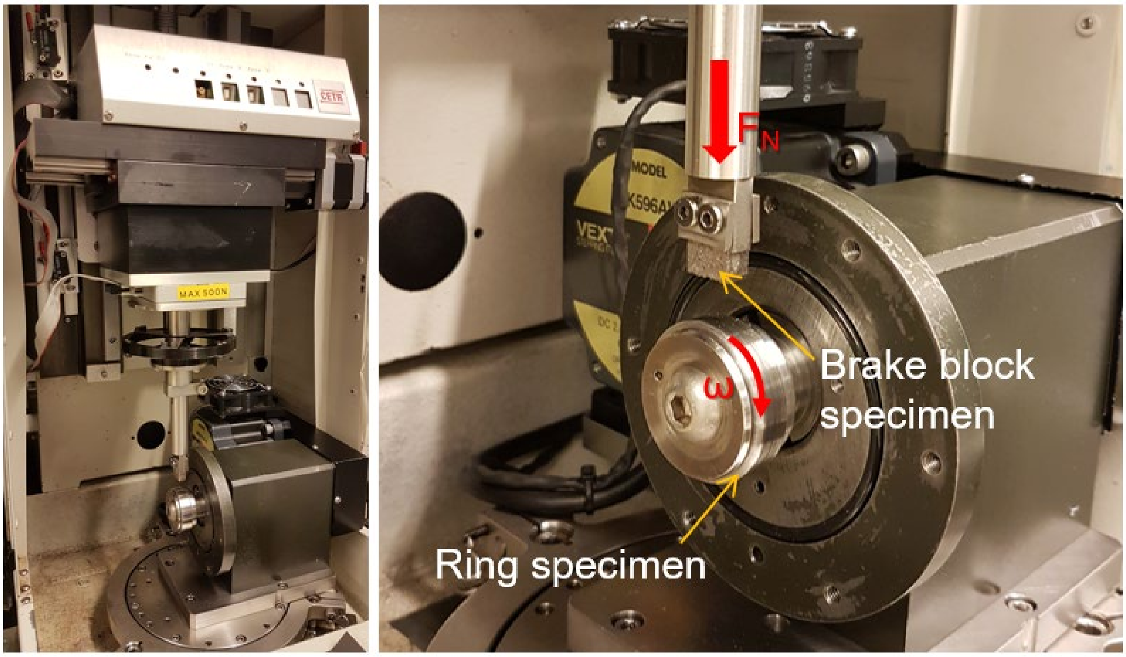

Figure 9. The block-on-ring test set up (left) and close-up of the test specimen mounted in the test rig (right).

The test parameters are given in Table 2. The test is initiated by starting the rotation of the ring specimen and thereafter applying the normal load to engage the block with the rotating ring. In these tests, the block and ring specimens were first run in for a period of 300 s corresponding to a sliding distance of 825 m. The test was then stopped and restarted without manipulating the test specimens. The second part of the test was 1000 s corresponding to 2750 m sliding distance.

Table 2. Test parameters used for the block-on-ring tests.

Parameter	Value
Load	5 N
Contact pressure (Hertzian line contact)	30 MPa
Sliding speed	2.75 m/s
Rotational speed	1500 rpm
Duration	300 + 1000 s
Sliding distance	825 + 2750 m
Temperature	R.T. (23 °C)
Relative humidity	20 – 30%

3.3 Pin-on-disc tests

The pin-on-disc tests were conducted using pin specimens of Ø6 mm and 8 mm height and disc specimens of Ø50 mm. The appearance of the different test specimens after manufacture can be seen in Figure 10.

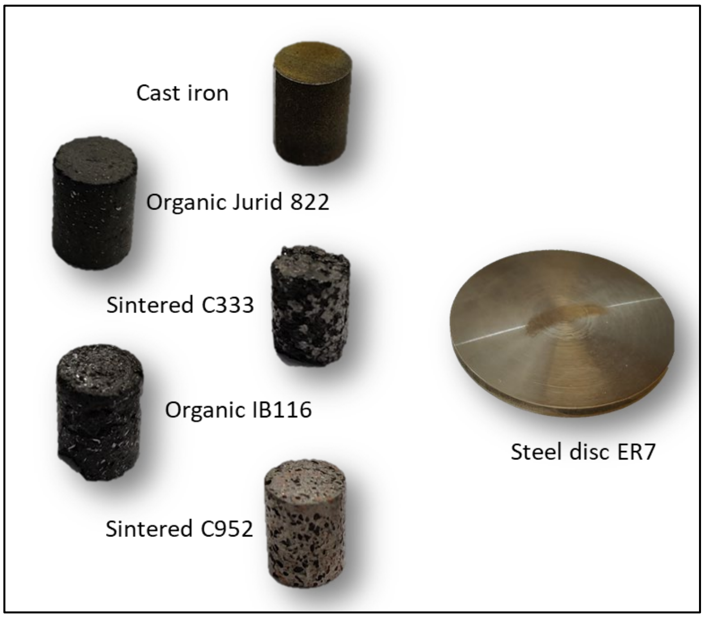

Figure 10. The pin specimens and the disc counter surface for the pin-on-disc tests

The tests were conducted by means of an Rtec MVT2 tribometer, Figure 11. In this tribometer, the upper pin specimen, which incorporates a load cell for measurement of the friction force and control of the applied normal force is loaded against the counter specimen. The disc specimen is clamped onto a rotating drive, which can be actively cooled by liquid nitrogen or heated by resistive heating. The tribometer incorporates a chamber for environmental control, which allows vacuum testing.

Two types of tests were conducted per brake material. One was under vacuum conditions, and the other was in atmospheric conditions with a relative humidity of 25-35%. The vacuum conditions give an indication of the friction behaviour of the brake materials at low temperature without influence of ice or oxide formation, whereas the tests with room atmospheric conditions allow the formation of ice on the surface during the tests, and thus, gives an indication of the friction behaviour under icy conditions.

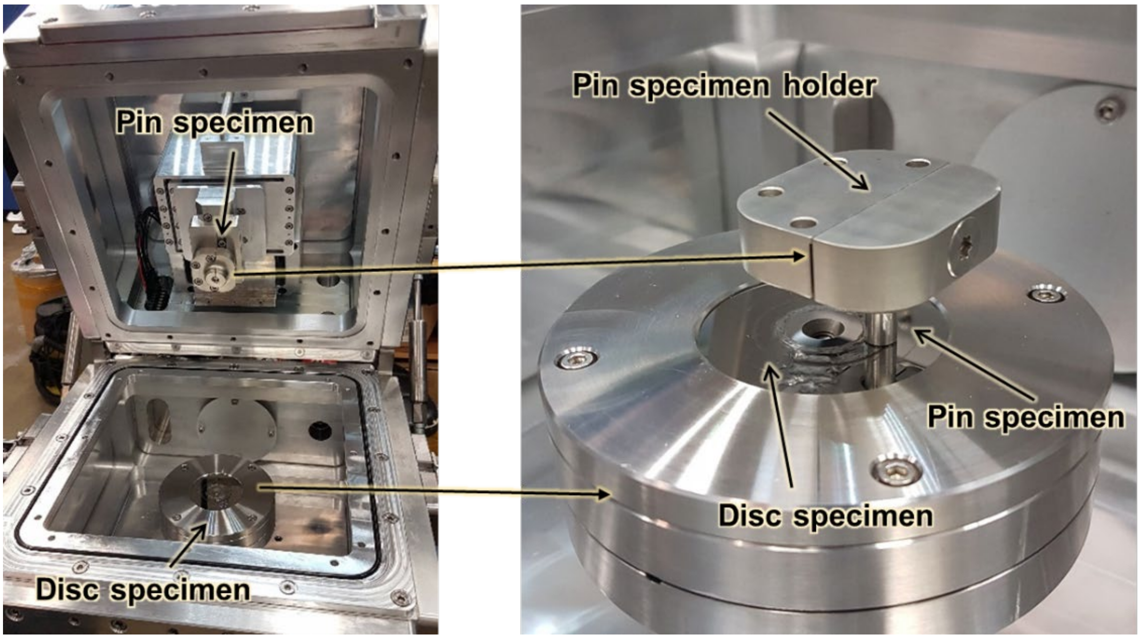

Figure 11. MVT-2 low temperature and vacuum tribometer.

For the test, the lower drive is initially taken to the corresponding rotation speed. The upper specimen is then loaded onto the lower specimen until the desired load is reached. In these tests, an initial running-in step was conducted for a sliding distance of 500 m, this was done at room temperature in order to accommodate the surfaces to one another. The chamber was in vacuum for the tests in vacuum and in normal atmospheric conditions for the tests under icy conditions. After the running-in, the specimens are disengaged, and cooling is initiated. Only the lower specimen is cooled down and the specimen rotates while cooling. Once the desired temperature of -15 °C was reached, the upper specimen was once again engaged, and the test was run for a total sliding distance of 1000 m. A photo of the test chamber after ice formation and engagement of the pin against the disc is shown in Figure 12.

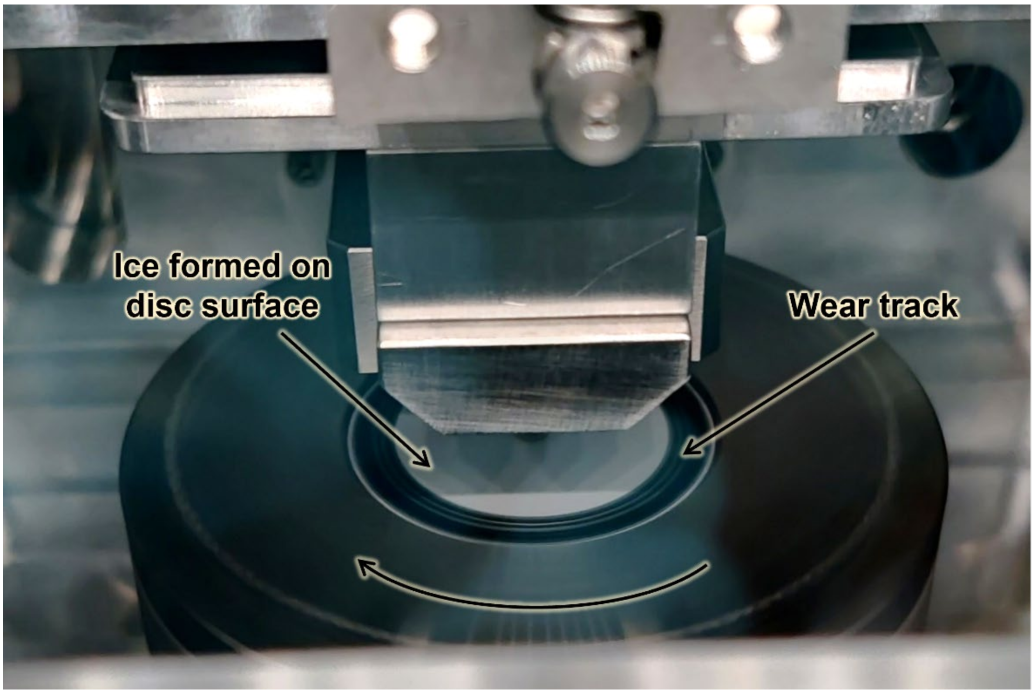

Figure 12. Photograph of the test chamber after cooling of the disc is completed, an ice layer has formed, and the pin specimen is engaged for the friction test.

The detailed test parameters used for the experiments are given in Table 3. The tests included an initial running-in step of 500 m to accommodate the surfaces to one another. The running-in step was done in all cases at room temperature, and it was done either in vacuum or in room atmospheric conditions accordingly.

Table 3. Test parameters used for the pin-on-disc tests.

Test parameter	Value
Load	10 N
Contact pressure	0.35 MPa
Sliding speed	2.3 m/s
Temperature	-15 °C
Sliding distance	500 m running-in + 1000 m test

3.4 Water absorption measurements

The experiments to investigate the water absorption for the porous CBB materials were performed by submerging two brake block specimens of each type (from the block-on-ring tests) in separate glass beakers filled with distilled water. The samples stayed submerged in water for 72 hours at room temperature (~22 °C). Thereafter, the samples were dried in air until they reached a stable weight (~1 hour), indicating the completion of the drying process. To quantify the absorbed water, the samples were weighed before and after the water exposure.

3.5 Analysis techniques

The surfaces topography of the specimens was analysed by means of a 3D optical interferometer WYKO NT 1100. All the specimens were analysed before and after the tests for the Block-on-ring tests.

The hardness of the rings and discs after manufacturing was measured using a Matsuzawa MXT-CX micro-hardness tester, using 300 gf as load and loading time of 15 seconds.

Optical microscopy was done using a Dino-Lite digital microscope in order to evaluate the contact area after the block-on-ring tests and calculate the nominal contact pressure.

The weight measurements for the water absorption analysis were conducted using a precision balance with a resolution of 0.01 mg.

4. Results and discussion

The following sections present and discusses the obtained results.

4.1 Surface topography before tribotesting

The surface topography of the as-delivered rings and the discs can be seen in Figure 13. These specimens had a defined topography with parallel grooves. In both cases, sliding was done parallel to the orientation of the grooves. The surface roughness (Sa) measured prior to the tribological tests was 0.930 µm for the rings and 0.350 µm for the disc specimens.

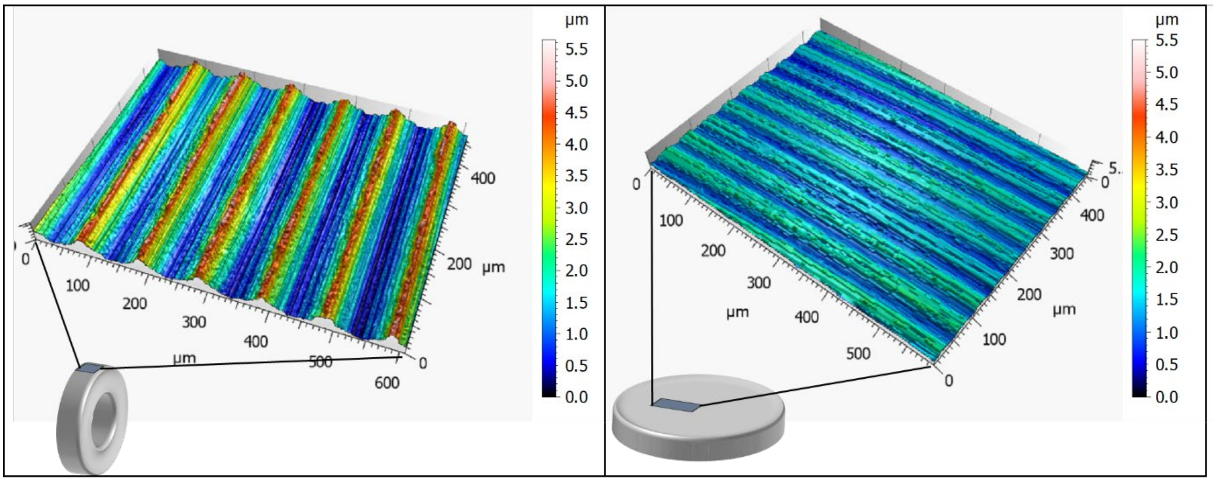

Figure 13. Surface topography of the steel wheel specimens. Ring specimen (left), disc specimen (right).

The topographies of the brake block materials after being manufactured can be seen in Figure 14. The different materials had different surface topographies after manufacturing. Cast iron had the highest surface roughness (Sa), 4.22 µm. Of the sintered CBB materials, the C333 material exhibited a higher Sa value (3.31 µm) compared to the C952 specimen (1.71 µm). A similar case was observed for the organic materials, where J822 was higher in roughness (3.27 µm) compared to the IB116 specimen (1.78 µm). It is important to note that no specimen showed a preferential orientation of the surface, as was the case for the steel counter surfaces discussed before.

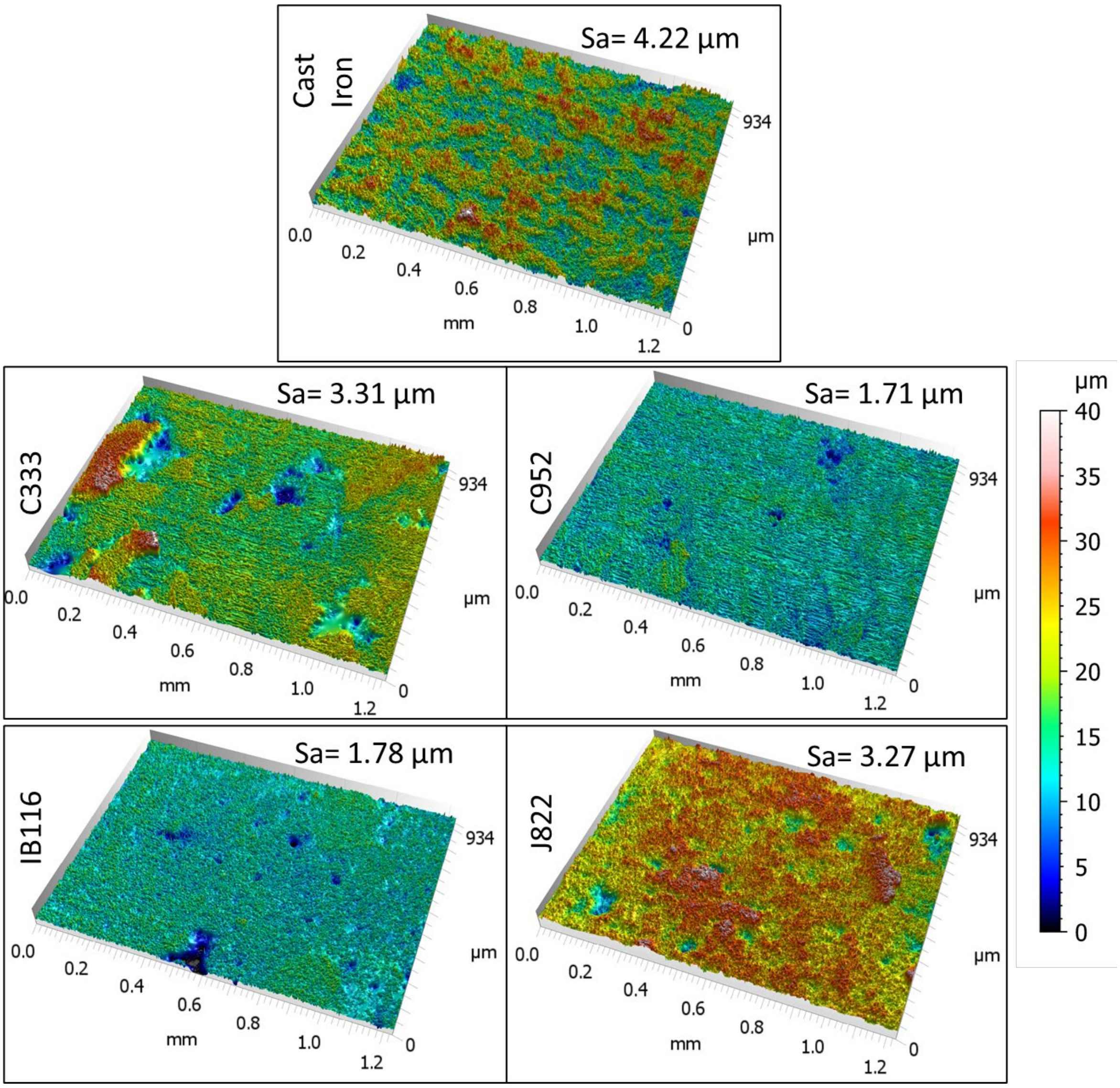

Figure 14. Surface topography of the brake material specimens.

4.2 Friction and wear behaviour in dry conditions

Figure 14 shows the friction behaviour during running in (Figure 15 (a)) and during the longer duration test (Figure 15 (b)) for all five brake block materials during sliding against the ER7 steel ring. The cast iron shows some scatter in the friction level, especially during running in. After running-in the friction is more repeatable and among the highest, showing coefficient of friction (CoF) values >0.3. The IB116 organic CBB shows very low and very repeatable friction behaviour. The friction coefficient is around 0.05 in steady state conditions. The Jurid 822 organic type K material shows relatively stable friction and the CoF is just below 0.2 in steady state conditions. When it comes to the sintered materials, the C333 type K material shows a large variation in CoF during running-in but a repeatable friction behaviour once the block and ring surfaces have been run in and accommodated to each other. The CoF in steady state is around 0.2 - 0.25, which is higher than the organic type K and expected based in the information in Table 1. The sintered type LL material C952 showed a rather high friction level close to 0.3 in steady state which is significantly higher than that for IB116. According to Table 1, the type LL material should have very similar friction. However, the friction level of C952 is similar to that of the cast iron. The type LL organic material (IB116) is supposed to have lower CoF than the type K material (J822), which is seen in these results, but it deviates significantly from the sintered type LL (C952). This may be due to the test conditions (higher contact pressure and lower sliding speed) compared to the actual application. It is also known that cast iron shows an increasing friction with reduced speed [2] which may be a reason for the higher CoF measured for the cast iron specimens in these tests.

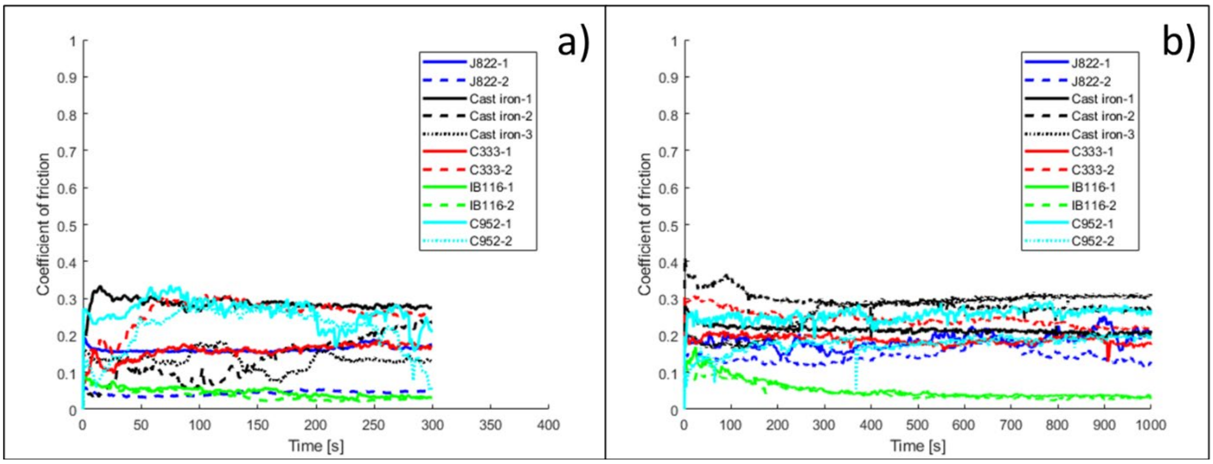

Figure 15. Coefficient of friction as a function of time for (a) the running-in tests and (b) the long duration tests.

As a comparison between the different brake block materials, the average coefficient of friction was calculated (Figure 16). This is the average of all the tests for each material and including the running-in and long duration part of the tests. The trends are the same as shown in Figure 15 with the lowest and most repeatable friction for IB116 followed by J822. The cast iron shows the highest friction and the two sintered CBB materials (C333 and C952) show very similar friction levels.

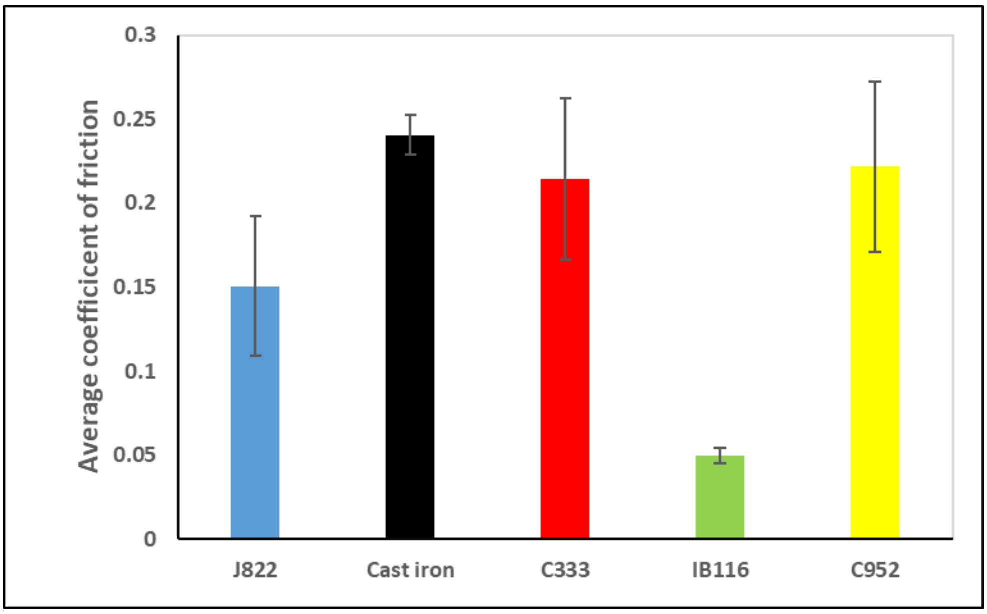

Figure 16. Average coefficient of friction from block-on-ring tests.

Wear of the specimens varied significantly depending on which materials were in contact. In Figure 17 the relative mass loss measured after the tribological tests can be seen. The relative mass loss is calculated as the mass loss of the specimen relative to its initial weight. This presentation of the data was chosen due to the large variation in density of the different brake block materials. As seen, the CBB materials that underwent the most significant wear were the type K sintered C333, followed by the organic J822. On the other hand, the type LL brake materials had similar relative weight loss, but these two materials had significant difference concerning their friction behaviour. In terms of wear of the wheel steel, this specimen undergoes the most significant wear after interaction against the sintered type LL C952 and the cast iron.

Due to the relatively small quantities of wear debris generated in these laboratory tests, it was not possible to conduct an analysis of the particle size and composition. For this purpose, it is recommended to perform laboratory brake tests using full-scale wheels and blocks to generate sufficient amount of wear debris that can be collected and analysed.

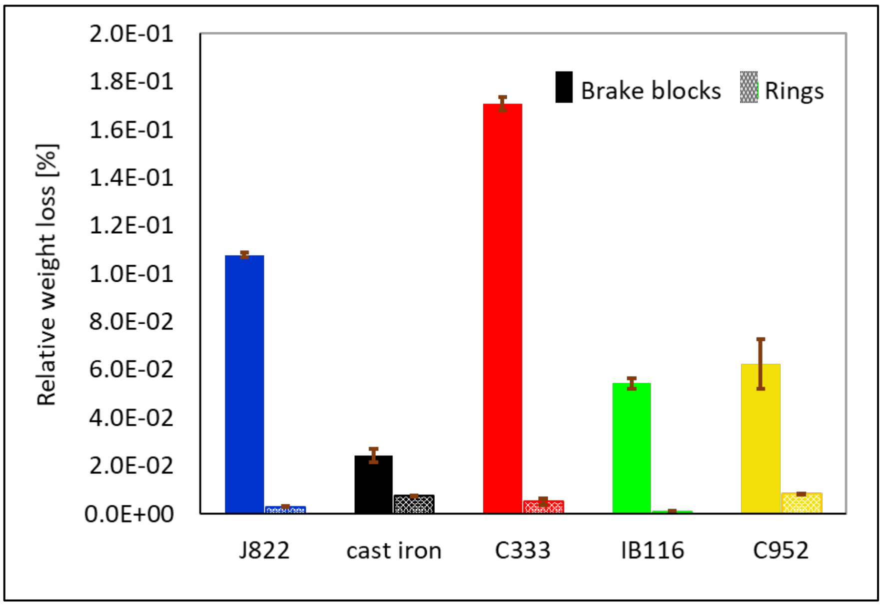

Figure 17. Relative weight loss of the specimens after the tribological tests.

Since the friction coefficients differ between the different brake block materials when sliding against steel, the friction power per area will also vary between the different tests. Therefore, the average absolute weight loss of the specimens were normalised with respect to the friction power per area which was calculated as

$$\frac{P_f}{A} = \frac{\mu \cdot F_N \cdot v}{A}$$

where P_f is the friction power, A is the contact area measured after the test using optical microscope, μ is the average coefficient of friction, F_N is the normal load, and v is the sliding velocity.

Figure 18 shows the normalised weight loss in $g \cdot m^2/W$. Since the mass loss is not normalised with the initial weight of the samples, deviations from data in Figure 17 can occur due to the different masses of the samples. This is especially seen for the relatively low weight of the CBB brake blocks compared to the relatively higher weight of the rings. The main difference to the relative weight loss (Figure 17) for the brake blocks is observed for J822 that show the lowest normalised wear. This can be attributed to a low mass loss of the J822 block specimen and therefore also a small contact area combined with an average friction which was the second lowest among the brake block materials. In case of the steel rings, it can be observed that the normalised wear for the ring sliding against the cast iron brake block increases, compared to the relative weight loss, and is higher than that for the cast iron block.

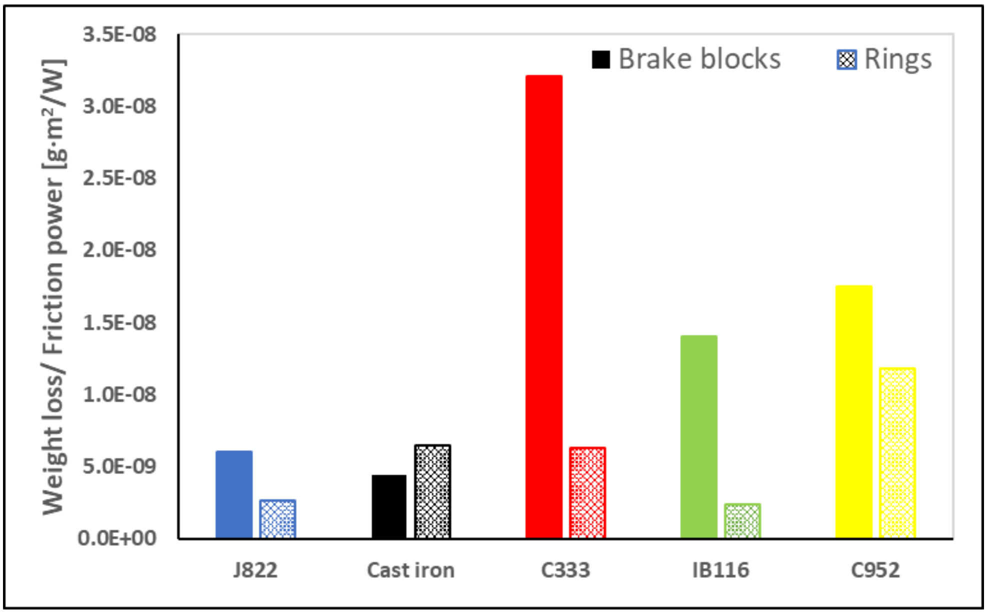

Figure 18. Absolute weight loss normalised with respect to friction power per area.

Due to the nature of the block-on-ring test configuration, the contact area will change as wear of the block specimen takes place. To investigate the final contact pressure for each material combination the wear scar on the block specimens were analysed using an optical microscope and the projected area was then calculated (Figure 19). The calculated contact pressures are shown in Figure 20, these vary between 0.3 - 0.6 MPa, which is in the same order of magnitude as in the real application (Table 1).

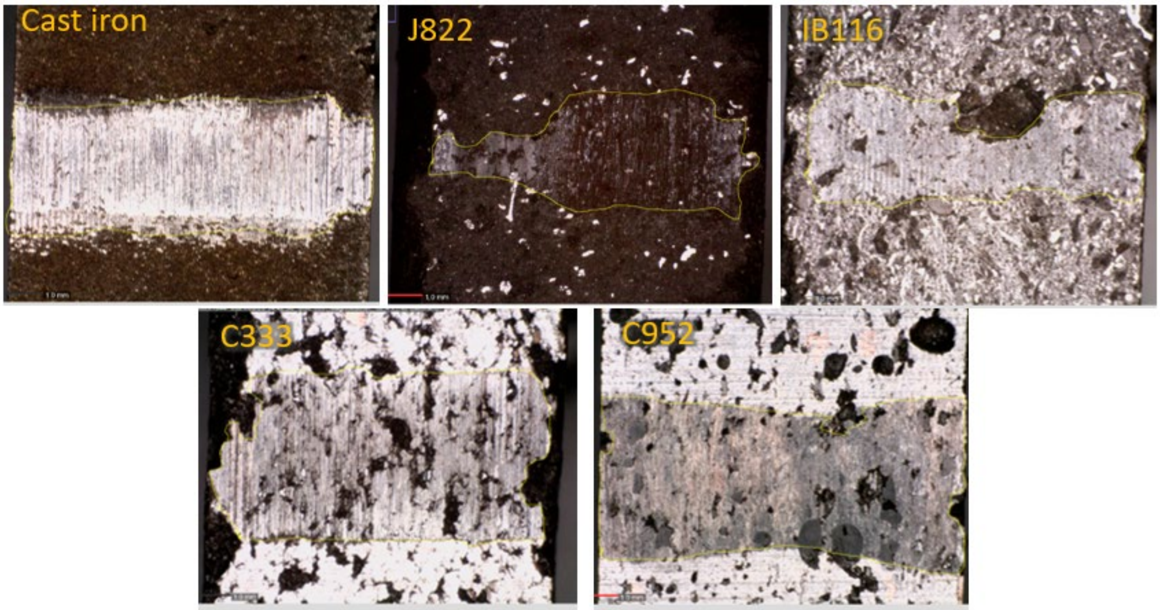

Figure 19. Representative optical micrographs of the block specimen wear scars.

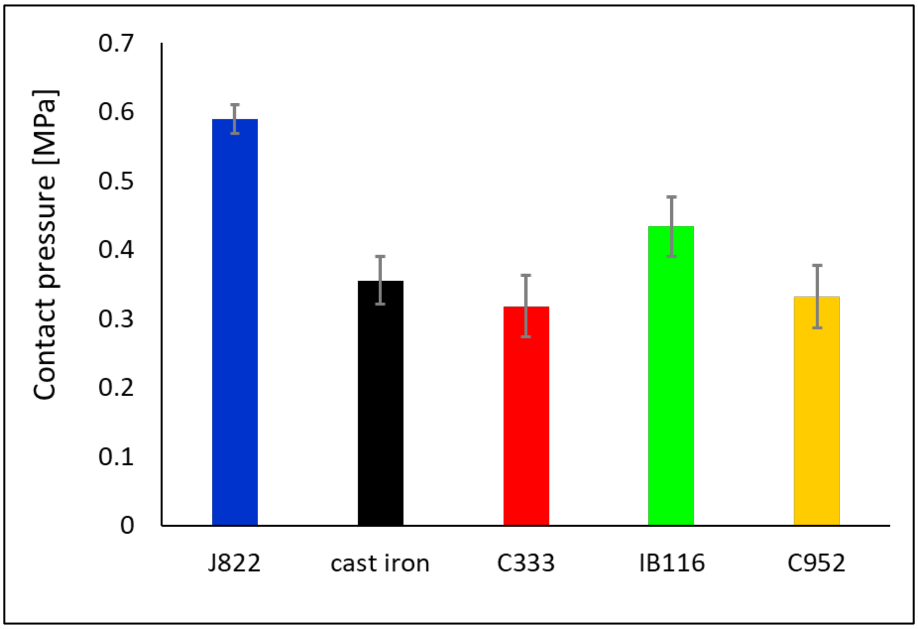

Figure 20. Contact pressure at the end of the block-on-ring tests.

Below, representative topography images of the worn surfaces are presented based on the type of brake material, i.e., reference cast iron, sintered CBB and organic CBB.

An example of the appearance of the topography of the cast iron block sliding against the wheel material is shown in Figure 21. Both surfaces underwent wear, the ring material underwent mild wear resulting in a slight smoothening of the surface asperities, as a change from 0.93 µm to ~0.50 µm was measured. In the case of the brake material, the surface developed a surface lay in the direction of sliding, which mirrors that of the ring. A significantly smoother surface was left after the tribological tests (~0.35 µm).

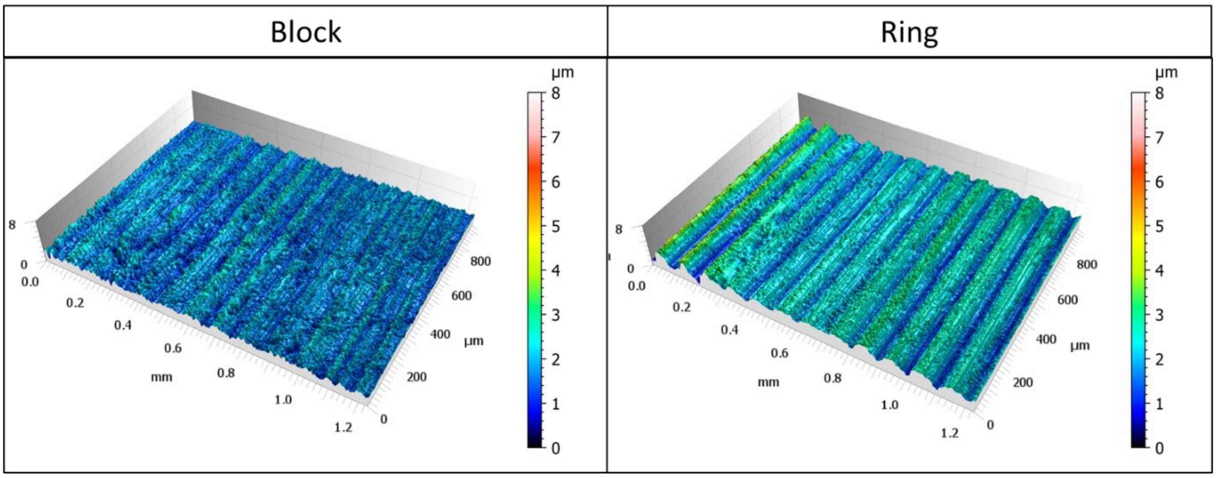

Figure 21. Surface topography of the block and ring specimens for the cast iron vs wheel steel

The surfaces of the specimens after the tribological tests with the sintered CBB materials are given in Figure 22. For the interaction between the type LL brake material C952 and the steel wheel, significant wear was observed in both the ring and the block specimens. The ring underwent significant wear and the topography changed as it developed fine grooves and a prominent waviness. The roughness varied significantly depending on where it was measured (from 0.30 to 0.70 µm). The C952 block developed a texture in the direction of sliding, with coarse grooves and high waviness. The surface roughness in this case, also varied significantly depending on the area of measurement, but in general it was above 1 µm, and it was significantly different compared to the initial surface.

Wear was also observed for the type K C333 specimen, but in this case, finer grooves were developed on the block, which mirrored those of the ring, which suggests milder wear for this pair of materials compared to C952. In both cases, slight build-up at the peaks of the asperities could be observed. The ring underwent a slight smoothening (~0.85 µm) whereas the block developed a surface topography with an average surface roughness of ~0.65 µm.

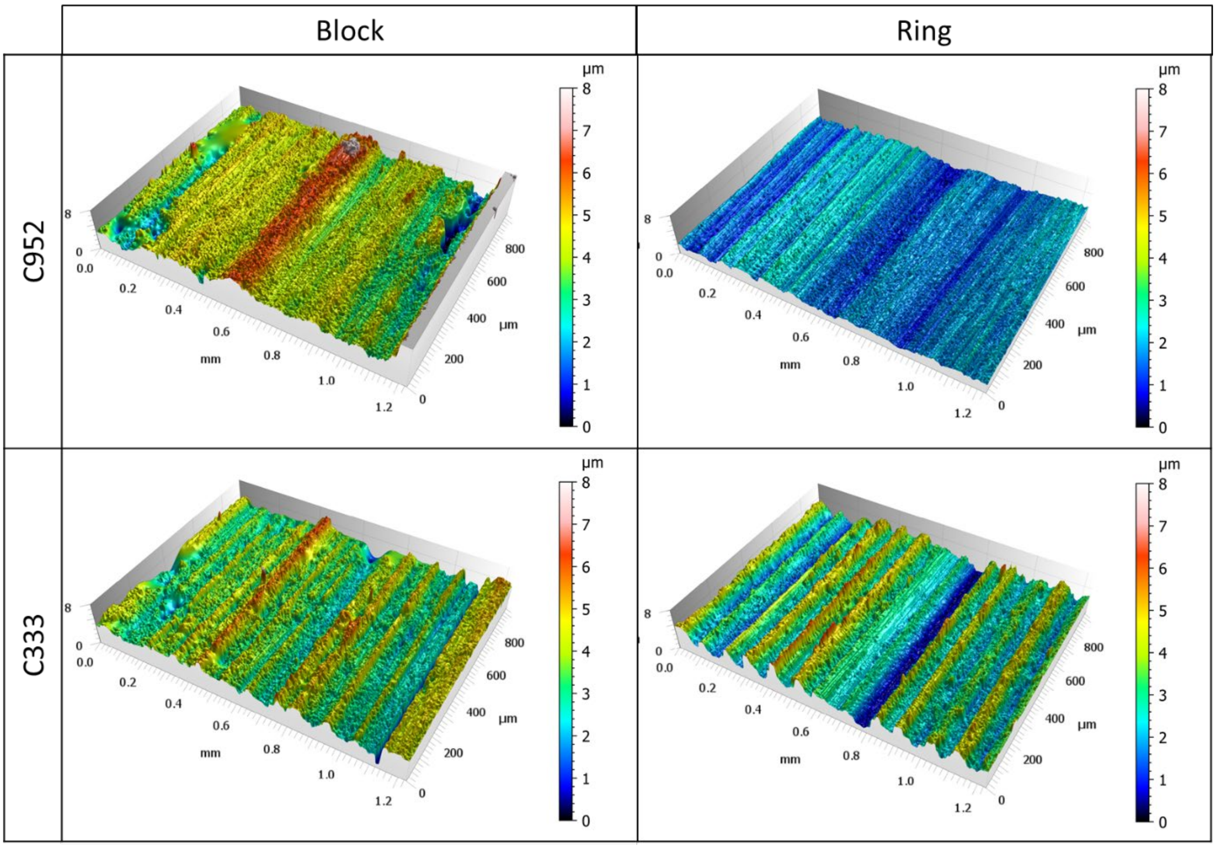

Figure 22. Surface topography of the block and ring specimens for the C952 (top) and C333 (bottom) vs wheel steel

The surface topography of the organic CBB materials is presented in Figure 23. For the tests with the type LL IB116 specimen, the surfaces underwent mild wear. Small grooves that mirror the surface of the ring can be observed on the block specimens. The surface of the ring remained largely unaffected, only minor instances of build-up, likely due to material transfer, could be observed at the peaks of the groves. The measured surface roughness after the test was ~0.35 µm and ~0.93 µm for the block and the ring respectively. The CBB specimen underwent clear smoothening, however, the surface did not develop a pronounced surface lay after the tests, as it was the case for all of the other CBB materials. This is also consistent with the very low friction measured for this material combination.

Regarding the interaction between the type K J822 CBB and the wheel material, mild wear of the ring was observed, with instances of material transfer. The measured surface roughness varied between 0.70 and 1 µm. The block developed a surface lay mirroring the ring surface, and the final surface roughness was measured between 1.0 and 1.6 µm.

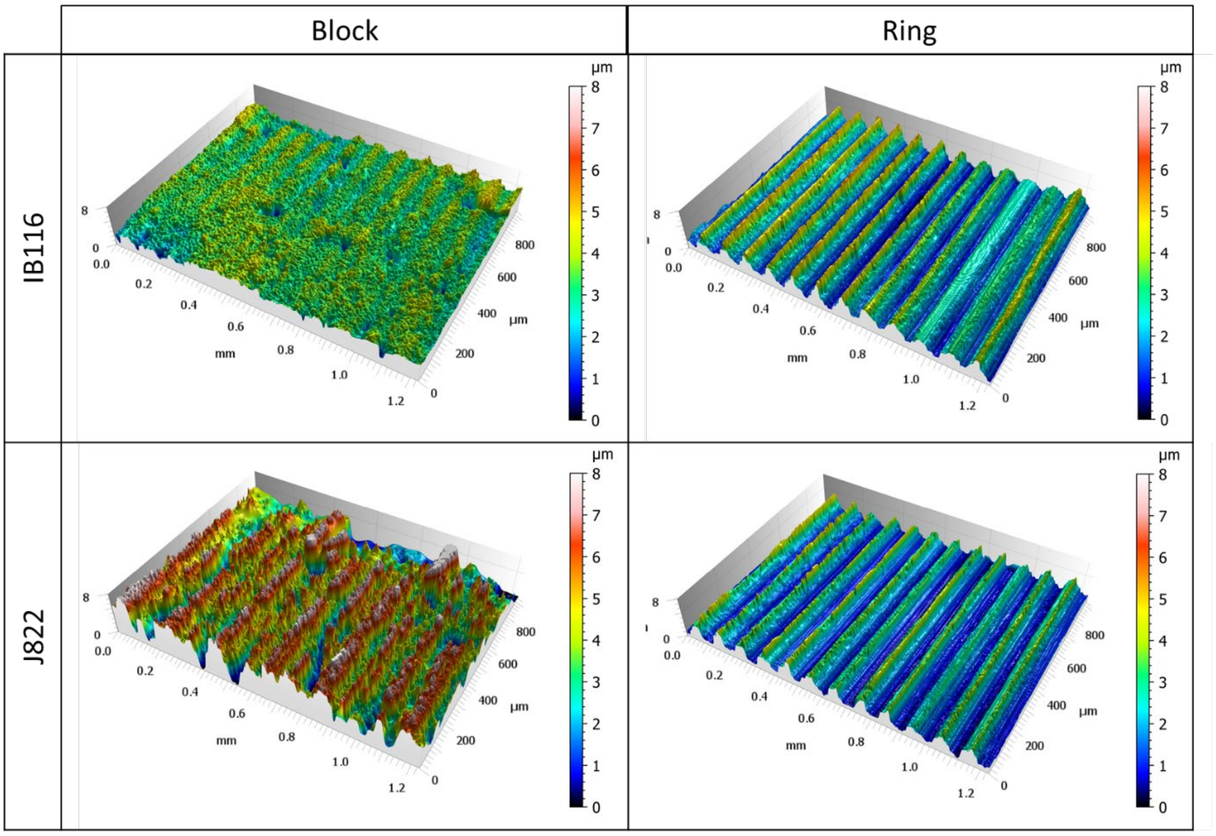

Figure 23. Surface topography of the block and ring specimens for the IB116 (top) and J822 (bottom) vs wheel steel

4.3 Friction behaviour in sub-zero conditions

Low temperature tests were done in order to evaluate the influence of temperature on the friction behaviour and to understand the influence of ice formation on the friction performance. In Figure 24, the average friction coefficients of all the tested materials in vacuum and icy conditions are shown. As seen, under vacuum condition, the friction coefficient was the highest for the cast iron (0.65) followed by the sintered materials, C952 (0.57) and C333 (0.58), type LL and type K respectively. The organic materials had the lowest friction coefficient, with the type LL IB116 material being the lowest (0.25), and type K J822 being the highest (0.35). These values give an indication on the effect of temperature on friction for cast iron as well as different CBB materials without any influence from oxidation and other contaminants such water and/or ice. Under icy conditions, all of the materials showed low coefficients of friction, where the cast iron and the type LL organic IB116 material were the lowest at 0.045 and 0.041 respectively. The type K J822 had a slightly higher coefficient of friction (0.049). In this type of condition, the materials with the highest friction coefficient were the organic materials, where type K C333 was the highest (0.098) followed by type LL C952 (0.057).

These results indicate that the nature of the CBB material, whether organic or sintered, has a more significant effect on how low or high the friction coefficient can be. It is important to note that in all of these tests, the temperature is constantly kept low with active cooling, which means that no significant influence from frictional heating takes place.

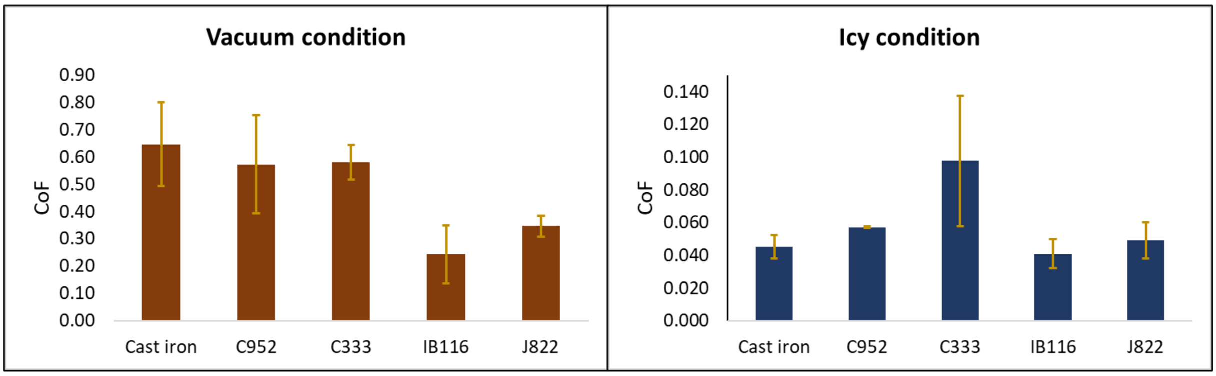

Figure 24. Comparison of the friction coefficient for the different brake materials at low temperature (-15°C). Vacuum (left) and Icy (right).

The behaviour of the friction coefficient as a function of time is exemplified and discussed below. In these figures, the grey part of the curve corresponds to the running-in period (500 m), which was done in all cases at room temperature. The following part of the curve corresponds to the test at low temperature (1000 m). In all cases, a representative curve from the three tests was selected for clarity.

Figure 25 shows the friction behaviour for the cast iron. As seen, during the running in period, the cast iron stabilises its friction coefficient at values around 0.5. In vacuum, it shows an increasing tendency with time, whereas in icy condition, it shows transitions from 0.04 to 0.07 throughout the entire duration of the test.

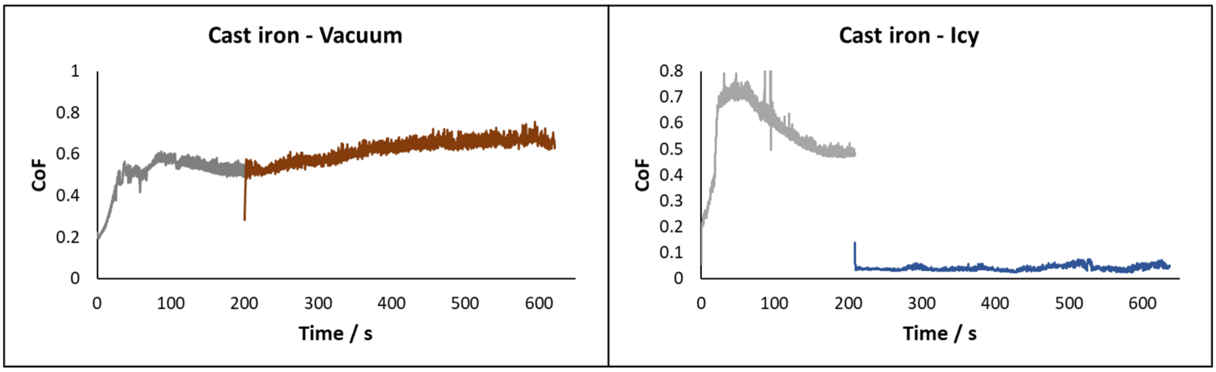

Figure 25. Evolution of the friction coefficient as a function of time for the cast iron at low temperature (-15°C). Vacuum (left) and Icy (right).

The evolution of the coefficient of friction with time for the sintered materials can be seen in Figure 26. These materials showed a relatively stable behaviour under vacuum conditions, after the running-in, friction did not change significantly and it quickly stabilised, particularly for the C333 CBB material. Under icy conditions, the behaviour was much more stable for the C952 material than it was for C333. The latter had significant changes in friction throughout the test, and it also showed more variance from test to test, where the friction coefficient varied from 0.05 to 0.15. This indicates that even though the average value is higher compared to other tests, this material can at times also experience similarly low coefficients of friction as compared to the other brake materials.

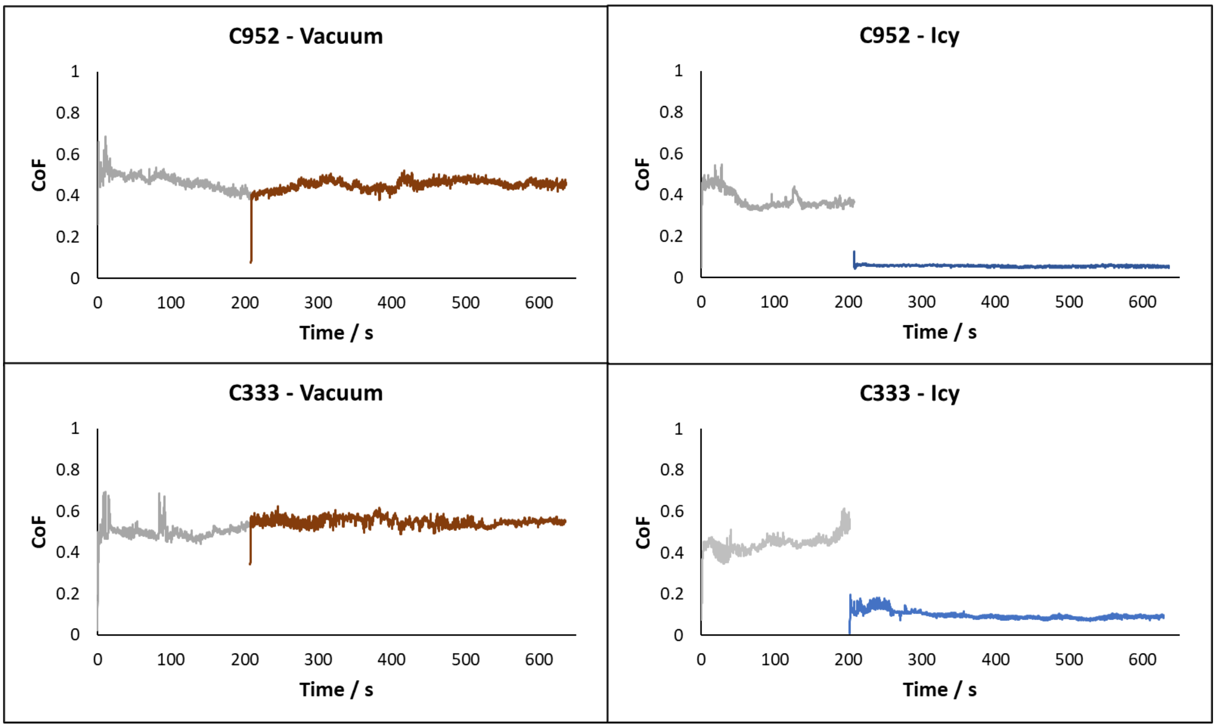

Figure 26. Evolution of the friction coefficient as a function of time for the sintered materials at low temperature (-15°C). Vacuum (left) and Icy (right).

In the case of the organic materials (Figure 27), stable and low friction was observed under vacuum. Type LL IB116 had a reducing tendency with time, whereas type K J822 remained stable. Under Icy conditions, the coefficient of friction varied throughout the test within a range of 0.03 to 0.07 for IB116 and from 0.025 to 0.09 for J822.

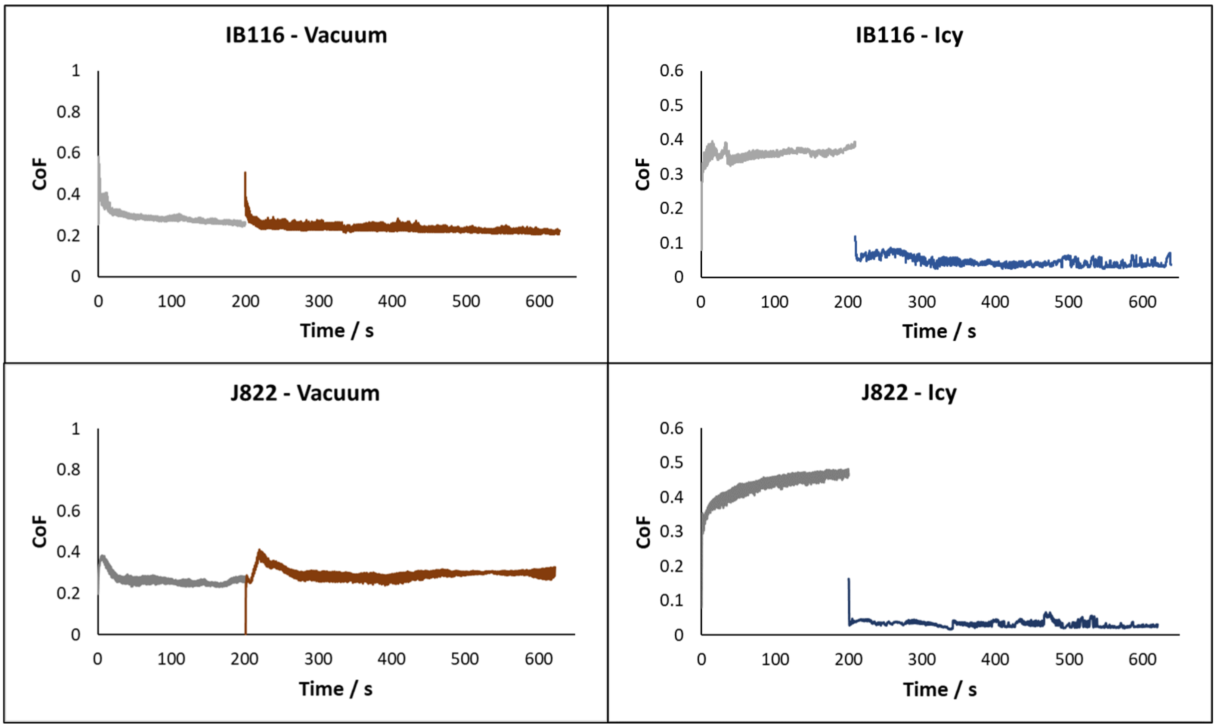

Figure 27. Evolution of the friction coefficient as a function of time for the organic materials at low temperature (-15°C). Vacuum (left) and Icy (right).

It should be noted that since the disc specimen is actively cooled, the preferential surface for ice formation is going to be there. As the brake material pin is engaged with the cold rotating disc with an ice layer on, it is likely to slide against ice initially. The low friction values are hence due to the brake material – ice contact. However, any variation in friction is a sign of temporary removal or rupture of the ice layer and hence an indication of the ability of the CBB material to function in icy conditions.

4.4 Water absorption

Figure 28 shows the glass beakers with distilled water after the brake block materials had been kept submerged for 72 hours at room temperature. It is clear that all brake block materials, except Jurid 822, experience some degree of corrosion as seen by the discoloration of the distilled water. This is likely due to contents of iron in the CBB materials.

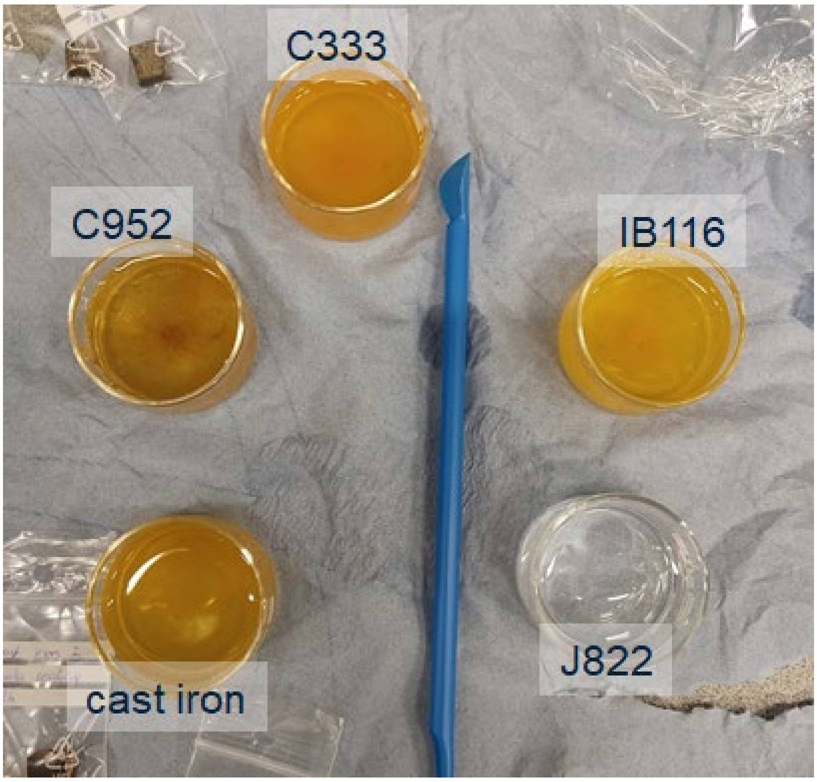

Figure 28. Appearance of the distilled water after soaking the brake block materials for 72 hours.

The measured weight change of the brake materials after soaking in distilled water is shown in Figure 29. The CBB materials C333, C952, and IB116 show very similar absorption of water whereas J822 shows more than four times higher water absorption. The cast iron shows a small weight loss due to corrosion. This is an interesting finding, which indicates that the CBB materials, due its inherent porosity, are capable of retaining water, which may then promote ice layer formation. Frictional heating during breaking will obviously remove retained water, but since the temperature of the organic CBB materials does not increase significantly due to its low thermal conductivity, any absorbed water may remain in the material.

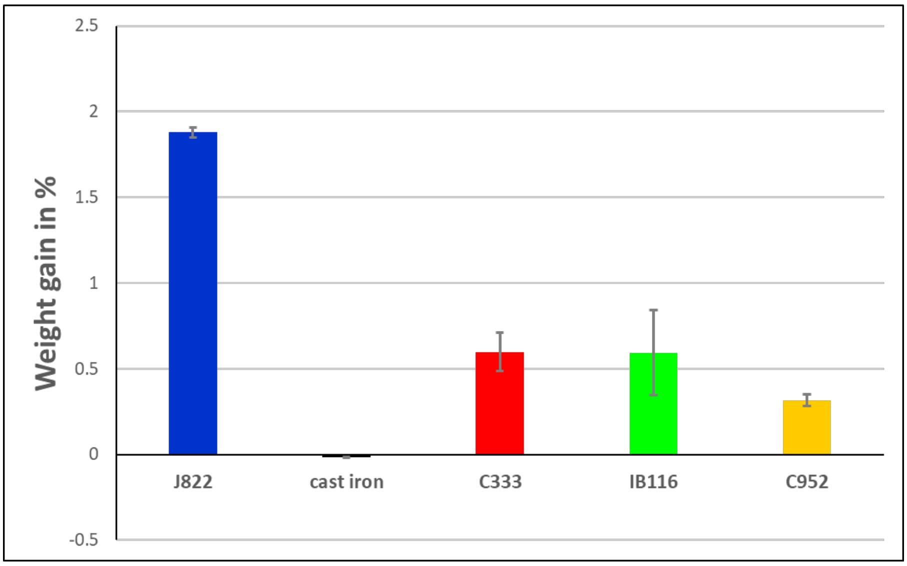

Figure 29. Weight change in percent of the initial weight of the brake block material after 72 hours soaking in distilled water.

5. Concluding remarks

The tribological behaviour of five different brake block materials (cast iron, two organic CBB, and two sintered CBB) have been studied in ambient conditions using a block-on-ring test and in low temperature conditions with and without vacuum using a pin-on-disc test. The main remarks from this study are:

1. The block-on-ring test is capable of differentiating between the tribological behaviour of the different brake block materials during sliding against steel.
    a. In dry conditions at room temperature, cast iron shows a relatively high and stable friction coefficient. The type K CBB materials (J822 and C333) show repeatable friction behaviour. The type LL CBB materials (IB116 and C952) show considerably different friction behaviour with very low values and good repeatability for IB116, and higher friction with more scatter for C952.
    b. Wear of the brake block materials at room temperature and dry conditions was highest for the type K and lowest for the type LL CBB materials. Highest wear on the steel counter surface was induced by cast iron and C952.
2. The low temperature pin-on-disc tests were able to characterise the friction behaviour of the brake block materials in sub-zero temperatures in dry and icy conditions.
    a. Friction levels at –15 °C and vacuum conditions were similar for the cast iron and sintered CBB materials whereas it was lower for the organic CBB materials.
    b. At –15 °C and humid atmosphere, resulting in ice formation, friction was highest for the sintered CBB (especially C333) and similar between cast iron and organic CBB.
    c. In sub-zero conditions, the friction behaviour is significantly influenced by the nature of the CBB materials. Sintered materials showed higher friction values both in dry and icy conditions.
3. Water absorption measurements showed that all CBB materials have the possibility to retain water in the porous structure. The organic type K J822 material showed four times higher water absorption than the other materials.
4. The tribological tests have shown that sintered CBB materials results in higher friction at low temperatures, which can be correlated to the improved performance of these materials under winter conditions, as seen from field test experience.

6. Future work

This study has shown the potential of using laboratory tribological tests as a tool for screening and ranking of brake block materials with respect to their friction and wear performance. It has also contributed to increasing the understanding about the friction and wear behaviour under comparable and repeatable operating conditions.

Future studies in this area could focus on the following topics:

- Effect of water absorption in CBB materials on friction behaviour under low temperature conditions.
- Influence of normal load on friction between CBB brake block materials and steel in presence of ice.
- Study the effect of surface topography of the steel surface on friction during running-in and steady state running conditions.
- Material characterisation (mechanical properties, microstructures, composition using e.g. nanoindentation, scanning electron microscopy, energy dispersive spectroscopy, X-ray diffraction) of worn brake blocks from field use in order to increase the understanding about how the CBB materials degrade and what the properties of the worn surfaces and near surface regions are.

References

[1] https://www.globalrailwayreview.com/article/1164/uic-activities-on-composite-brake-shoes/ {Acc. 2021-09-27}
[2] S. Teimourimanesh et al., 16th International Wheelset Congress (IWC16), Cape Town (RSA) March 2010
[3] Report Swedish Transport Agency ”Risk assessment regarding composite brake blocks during Swedish winter conditions” (Ref TSJ 2019-5343)
[4] http://railway-research.org/IMG/pdf/760.pdf {Acc. 2021-09-27}